Nonequilibrium velocity distribution function of gases: Kinetic theory and molecular dynamics

Werner Loose and Siegfried Hess
Institut für Theoretische Physik, Technische Universität Berlin, PN 7-1, D-1000 Berlin 12, West Germany
(Received 22 June 1987)

In the first part of this paper the moment method is employed to solve the nonlinear Boltzmann equation. An expansion about a local Maxwellian distribution is used with the basis functions introduced by Waldmann [in *Handbuch der Physik*, edited by S. Flügge (Springer, Berlin, 1958), Vol. 12, p. 295]. Earlier approaches are extended by the inclusion of more expansion functions (Sonine polynomials) in order to obtain an approximation for the velocity distribution function. General relations for the coupling of the moments are derived and the resulting transport relaxation equations are solved for the special Couette geometry. The influence of the higher moments on the viscosity coefficients is small, but the higher moments are essential for the distribution function itself. The inclusion of the quadratic collision matrix elements leads to minor modifications only. In another part of the paper the velocity distribution function is obtained from nonequilibrium molecular dynamics. Excellent agreement with the predictions of the moment method is found provided that the constant temperature constraint of the simulation is taken into account by incorporating a nonconservative external force term into the Boltzmann equation. The effect of this modification is discussed in detail for the viscosity coefficients. The non-Newtonian flow behavior of gases is studied on the microscopic level of the velocity distribution function. In addition an isotropic distortion of the Maxwellian distribution is observed.

I. INTRODUCTION

Within the framework of kinetic theory, the pressure tensor of a gas is determined by an integral over the nonequilibrium velocity distribution function.[1,2] The viscosity, defined as the ratio of a (nondiagonal) element of the pressure tensor and the shear rate, provides indirect evidence for its distortion by a viscous flow. The velocity distribution function, of course, contains more information on the microscopic mechanism underlying the nonequilibrium process than the transport coefficient. The experimental determination of the distortion of the velocity distribution function by a transport process via Doppler broadening[3] is rather difficult; for the case of a heat-conducting gas see Ref. 4. Here, molecular dynamics can provide the desired data from a simulation of a nonequilibrium experiment. First results for the linear-flow regime were reported in Ref. 5.

This article is devoted to an analysis of the velocity distribution function and its relation to the viscosity for a gas undergoing a plane Couette flow. We proceed as follows. In Sec. II the kinetic theory based on the Boltzmann equation is reviewed briefly. A modified moment method[1] is employed to derive an infinite set of coupled equations for the moments, referred to as transport relaxation equations. The moments are the coefficients in an expansion of the velocity distribution function about a local Maxwellian. The expansion functions (Sonine polynomials), however, are known. To obtain the nonequilibrium velocity distribution, the transport relaxation equations have to be solved for the moments. For this purpose an appropriate closure is chosen in Sec. III. Since here the goal is to get an approximation for the distribution function itself, earlier approaches[6] are extended by including more expansion functions. The theory is also capable of describing phenomena nonlinear in the shear rate. In Sec. IV the transport relaxation equations are stated explicitly for the plane Couette geometry.

The comparison of the kinetic theory with results from nonequilibrium molecular dynamics (NEMD) is an essential point of this article. The basic ideas and the problems arising from the imposed constraints are discussed in Sec. V. It turns out that the constant temperature constraint requires a modification of the Boltzmann equation, insofar as a nonconservative "drag" force has to be added.

In Sec. VI the viscosity coefficients obtained from solutions of the Boltzmann equation with and without an additional force term are compared with results of the NEMD computer simulation. Excellent agreement can only be achieved by the inclusion of the external force. Furthermore, the higher moments can also be evaluated as N-particle averages from the simulation. The comparison with the solution of the transport relaxation equations is again satisfactory. Some insight into the effect of the quadratic collision operator is gained in addition.

The velocity distribution function itself can also be extracted from the simulation. The method and results for the linear-flow regime are presented in Sec. VII. Finally, in Sec. VIII the relation between the non-Newtonian flow behavior and the corresponding distortion of the distribution function is elucidated.

A few general remarks on nonlinear flow phenomena in fluids[7,8] are in order. Usually, rheology focuses on the rather complex flow phenomena of polymer melts, disper-

sions, and other, more exotic materials. The constitutive equations of these substances are nonlinear and lead to non-Newtonian behavior, such as shear thinning (or thickening) and normal pressure differences.

The shear-rate dependence of the viscosity is related to structural changes in the fluid, e.g., polymer chains align in flow direction. It is interesting to note that even simple fluids, constituted of spherical particles, can exhibit a similar non-Newtonian flow behavior. Again, it goes along with changes in the internal structure of the fluid. For dense fluids, where the dynamics is dominated by the pair interaction, the Kirkwood-Smoluchowski equation was used to calculate the distortion of the pair distribution function due to the shear flow.[9] The theory was also capable of describing non-Newtonian phenomena in simple liquids.[10] It is conjectured that the resulting constitutive equations can be employed in the description of more complex systems.

It is well known that kinetic gas theory also leads to non-Newtonian effects. More than 50 years ago Burnett calculated the nonlinear corrections for the friction pressure.[2] Here, in contradistinction to simple liquids, they are of kinetic origin; the "structural" changes occur in the velocity space. In addition, the Boltzmann equation provides a well-established theoretical basis for this density regime; thus comparisons with computer simulation results can be considered as tests for the algorithm used. The rheology of ideal gases has attained growing attention in the last years.[6,11,12] But, so far emphasis has been laid on the transport properties alone.

Usually, the occurrence of non-Newtonian phenomena in simple fluids is restricted to very high shear rates, beyond the order of magnitude which is accessible in real laboratory experiments. Consequently, computer simulations with nonequilibrium molecular dynamics are of great importance.[13] However, it is *a priori* uncertain how accurately the computer model mimics the real experiment. For the plane Couette flow, e.g., the viscous heat is removed by the moving boundaries which, in addition, drive the flow. In the corresponding computer model, on the contrary, no boundaries are present. A spatially constant temperature field and a linear velocity gradient are enforced by homogeneous algorithms. Details will be given at the appropriate point in this paper.

The question of comparability to real experiments has drawn some attention in the past. Dufty[14] showed that in general the transport properties of a system at constant temperature differ from those of a system, where viscous heating is allowed. Only for Maxwell molecules the same viscosity results for both cases. For general force laws estimates of the difference were given. Here, a detailed analysis of the constant temperature constraint is presented. Although the flow field in the two situations is the same, differences in the viscosities occur which are due to the different temperature fields. Ladd and Hoover,[15] on the other hand, have demonstrated the agreement of the distribution function for a Lorentz gas obtained from NEMD with an analytical solution of the corresponding Boltzmann equation, using a relaxation time ansatz. The full Boltzmann collision term is necessary for the pure gas studied here.

II. THE MOMENT METHOD

The velocity distribution function $f(\mathbf{r},\mathbf{c},t)$ describes the state of a pure monoatomic gas and depends on position $\mathbf{r}$, particle velocity $\mathbf{c}$, and on time t. The number density $n(\mathbf{r},t)$ is given by

$$n(\mathbf{r},t)=\int f(\mathbf{r},\mathbf{c},t)d^3c \ . \tag{1}$$

Similarly, the other macroscopic entities can be obtained as averages evaluated with the distribution function f.

The temporal and spatial variation of f is governed by the Boltzmann equation, which, in the most general case, reads

$$\frac{\partial f}{\partial t}+\mathbf{c}\cdot\nabla f+\frac{\partial}{\partial \mathbf{c}}\cdot(\mathbf{K}f)=\left[\frac{\delta f}{\delta t}\right]_{\text{coll}} . \tag{2}$$

For dilute gases the time dependence of the distribution function is separated into a term due to an external force $\mathbf{K}$, which may depend on $\mathbf{c}$, a term describing the free flight of the particles (called "streaming term," $\mathbf{c}\cdot\nabla f$), and a term due to collisions among them [called "collision term," $(\delta f/\delta t)_{\text{coll}}$].

Following the notation used in Ref. 6, the dimensionless (local) peculiar velocity $\mathbf{V}(\mathbf{r},t)$ is introduced by

$$\sqrt{2}c_0\mathbf{V}\equiv\mathbf{c}-\mathbf{v},\quad c_0\equiv\sqrt{k_BT/m} \ , \tag{3}$$

where $\mathbf{v}(\mathbf{r},t)$ is the average (streaming) velocity. It is useful to express the velocity distribution in terms of $\mathbf{V}$ rather than $\mathbf{c}$, so $F(\mathbf{r},\mathbf{V},t)$ is defined by

$$n(\mathbf{r},t)F(\mathbf{r},\mathbf{V},t)d^3V=f(\mathbf{r},\mathbf{c},t)d^3c \ . \tag{4}$$

Then the local Maxwellian distribution simply reads

$$F_M(V^2)=\pi^{-3/2}\exp(-V^2) \ . \tag{5}$$

It is normalized according to

$$\int F_M(V^2)d^3V=1 \ . \tag{6}$$

The temperature and the average velocity are given by

$$\tfrac{3}{2}k_BT(\mathbf{r},t)=\frac{m}{2}\int(\mathbf{c}-\mathbf{v})^2F_M(V^2)d^3V \ , \tag{7}$$

$$\mathbf{v}(\mathbf{r},t)=\int \mathbf{c}F_M(V^2)d^3V \ . \tag{8}$$

For the nonequilibrium velocity distribution the following ansatz is made:

$$F(\mathbf{r},\mathbf{V},t)=F_M(V^2)[1+\Phi(\mathbf{r},\mathbf{V},t)] \ . \tag{9}$$

Hence, the deviation from local equilibrium is expressed by the function $\Phi(\mathbf{r},\mathbf{V},t)$.

A scalar product $\langle AB\rangle$ of two functions A and B depending on $\mathbf{V}$ is defined by

$$\langle AB\rangle=\int ABF_M(V^2)d^3V \ . \tag{10}$$

Using this notation $\langle A\rangle$ is written for the (local) equilibrium average of a function A. The nonequilibrium average $\langle\langle A\rangle\rangle$ has to be evaluated with the distribution F. Using (9) one gets

$$\langle\langle A\rangle\rangle\equiv\int FA\,d^3V=\langle A\rangle+\langle A\Phi\rangle \ . \tag{11}$$

The normalization, the average velocity, and the temperature can be obtained by taking averages with the local Maxwellian distribution of the collisional invariants 1, $\mathbf{V}$, and V^2, respectively, cf. (6)–(8). Thus the second term on the rhs of (11) should not contribute to these averages, and the following orthogonality requirements for Φ can be inferred:

$$\langle \psi_i \Phi \rangle = 0 \quad \text{for } \psi_i = 1, \mathbf{V}, V^2 \ . \tag{12}$$

The deviation from local equilibrium $\Phi(\mathbf{r},\mathbf{V},t)$ is expanded with respect to orthogonal functions $\phi^i(\mathbf{V})$ according to

$$\Phi(\mathbf{r},\mathbf{V},t) = \sum_i a^i(\mathbf{r},t)\phi^i(\mathbf{V}) \ , \tag{13}$$

with

$$\langle \phi^i \phi^j \rangle = \delta_{ij} \ . \tag{14}$$

The expansion functions will be discussed in more detail in Sec. III. Note, the label i stands for a set of indices, as, in general, the functions $\phi^i(\mathbf{V})$ will be tensors.

The moments $a^i(\mathbf{r},t)$ are just the averages of the corresponding expansion functions ($\langle \phi^i \rangle = 0$), cf. (11) and (14),

$$a^i = \langle \Phi \phi^i \rangle = \langle\langle \phi^i \rangle\rangle \ . \tag{15}$$

In the following we restrict ourselves to the case of a stationary, isothermal, plane Couette flow ($\nabla \cdot \mathbf{v} = 0$). For this case the following transport relaxation equations for the moments a^i as derived from the Boltzmann equation read

$$\frac{d}{dt}a^i + \sum_j \left[C^{ij}_\lambda \nabla_\lambda + \omega_\lambda \Gamma^{ij}_\lambda + \gamma_{\lambda\kappa}\Gamma^{ij}_{\lambda\kappa} + K^{ij} + \omega^{ij} + \sum_k \tilde{\omega}^{\,i,jk} a^k \right] a^j = -2\gamma_{\lambda\kappa}\langle \phi^i V_\lambda V_\kappa \rangle + \frac{1}{\sqrt{2}mc_0}\left\langle K_\lambda \frac{\partial}{\partial V_\lambda}\phi^i \right\rangle \ . \tag{16}$$

The following definitions have been used:

$$C^{ij}_\lambda \equiv \sqrt{2}c_0 \langle V_\lambda \phi^i \phi^j \rangle, \quad \omega^{ij} \equiv \langle \phi^i \omega(\phi^j) \rangle \ , \tag{17}$$

$$\Gamma^{ij}_\lambda \equiv \langle L_\lambda(\phi^i)\phi^j \rangle, \quad \tilde{\omega}^{\,i,jk} \equiv \langle \phi^i \tilde{\omega}(\phi^j \phi^k) \rangle \ , \tag{18}$$

$$\Gamma^{ij}_{\lambda\kappa} \equiv \langle L_{\lambda\kappa}(\phi^i)\phi^j \rangle, \quad -\sqrt{2}mc_0 K^{ij} \equiv \left\langle K_\lambda \frac{\partial}{\partial V_\lambda}(\phi^i)\phi^j \right\rangle \ , \tag{19}$$

$$L_\lambda \equiv \epsilon_{\lambda\mu\nu} V_\mu \frac{\partial}{\partial V_\nu}, \quad L_{\lambda\kappa} \equiv \left\{ V_\lambda \frac{\partial}{\partial V_\kappa} \right\}^0 \ , \tag{20}$$

$\omega(\cdots)$ and $\tilde{\omega}(\cdots)$ are the linear and quadratic parts or the collision operator.[6]

The symmetric traceless part of a tensor is denoted by $\{\cdots\}^0$, e.g., the shear gradient is decomposed according to

$$\nabla_\lambda v_\kappa = \epsilon_{\lambda\kappa\tau}\omega_\tau + \gamma_{\lambda\kappa} \tag{21}$$

with $\gamma_{\lambda\kappa} \equiv \{\nabla_\lambda v_\kappa\}^0$ and $\omega_\tau \equiv \frac{1}{2}\epsilon_{\tau\lambda\kappa}\nabla_\lambda v_\kappa$. With a^i calculated from Eq. (16), the nonequilibrium distribution function is known according to (9) and (13). The external force $\mathbf{K}$ will be specified in Sec. V. Until then only the properties of the transport relaxation equations (16) in the absence of external forces are treated.

III. CLOSURE OF THE TRANSPORT RELAXATION EQUATIONS

The transport relaxation equations (16) constitute a highly coupled system of differential equations for the moments a^i, which has to be solved to obtain an approximation for the velocity distribution function in nonequilibrium. In the following, the most relevant moments have to be selected in order to find a closure, which is appropriate to describe the nonequilibrium distribution function itself, rather than the transport coefficient, which is only an average taken with this distribution.

Our choice is guided by the results of Ref. 6 and by observations made with nonequilibrium molecular dynamics computer simulations, as will be demonstrated later. First, let us turn in more detail to the expansion (13). Taking into account the tensorial character of the expansion functions it reads

$$\Phi(\mathbf{r},\mathbf{V},t) = \sum_{l=0}^{\infty}\sum_{r=1}^{\infty} a^{(r)}_{\mu_1\cdots\mu_l}(\mathbf{r},t)\phi^r_{\mu_1\cdots\mu_l}(\mathbf{V}) \ , \tag{22}$$

with

$$\phi^{r+1}_{\mu_1\cdots\mu_l} \equiv \left[\frac{r!(2l+1)!!1/2\sqrt{\pi}}{l!\Gamma(l+r+\frac{3}{2})} \right]^{1/2} (-1)^r \times S^r_{l+1/2}(V^2)\{V_{\mu_1}\cdots V_{\mu_l}\}^0 \ , \tag{23}$$

where $S^r_m(V^2)$ is a Sonine polynomial of degree r.[1] Note, an expansion with respect to irreducible tensors is used, which has the advantage of clearly indicating the symmetry of the directional distortion.

The orthogonality condition (14) now reads

$$\langle \phi^r_{\mu_1\cdots\mu_l}\phi^{r'}_{\nu_1\cdots\nu_{l'}} \rangle = \delta^{rr'}\delta_{ll'}\Delta^{(l)}_{\mu_1\cdots\mu_l,\nu_1\cdots\nu_{l'}} \ , \tag{24}$$

with the projection tensors $\Delta^{(l)}_{\cdots,\cdots}$.[16] For $l=2$

$$\Delta^{(2)}_{\mu\nu,\mu'\nu'} \equiv \tfrac{1}{2}(\delta_{\mu\mu'}\delta_{\nu\nu'} + \delta_{\mu\nu'}\delta_{\nu\mu'}) - \tfrac{1}{3}\delta_{\mu\nu}\delta_{\mu'\nu'} \tag{25}$$

and

$$\Delta^{(2)}_{\mu\nu,\mu'\nu'} A_{\mu'\nu'} = \{A_{\mu\nu}\}^0 \ , \tag{26}$$

for an arbitrary second rank tensor $A_{\mu\nu}$.

To select the appropriate moments it is useful to discuss the coupling due to the several terms in (16). Of special interest is the first expansion tensor of rank two,

$$\phi^1_{\mu\nu} = \sqrt{2}\{V_\mu V_\nu\}^0 \ . \tag{27}$$

In kinetic gas theory the friction pressure tensor $\{P_{\mu\nu}\}^0$ is given as

$$\{P_{\mu\nu}\}^0 = 2P\int F(\mathbf{V})\{V_\mu V_\nu\}^0 d^3V = 2P\langle\langle \{V_\mu V_\nu\}^0 \rangle\rangle \ , \tag{28}$$

cf. (11), with $P=nk_BT$. Hence, $\langle\langle \phi^1_{\mu\nu}\rangle\rangle$ is proportional to the friction pressure tensor. The corresponding moment, cf. (15), is denoted by $\pi_{\mu\nu}$, in order to stress its meaning as a dimensionless friction pressure tensor,

$$\pi_{\mu\nu}\equiv a^{(1)}_{\mu\nu}=\langle\langle \phi^1_{\mu\nu}\rangle\rangle=\{P_{\mu\nu}\}^0/(\sqrt{2}P)\ . \tag{29}$$

Due to the orthogonality condition (24), $\pi_{\mu\nu}$ is the only moment, for which the rhs of (16) is nonvanishing.

A coupling of tensors of odd rank and the driving term $\gamma_{\mu\nu}$ can only be achieved via the C^{ij}_{λ}-matrix elements. But for the plane (homogeneous) Couette flow, no gradients of the moments can occur; thus odd ranked expansion tensors need not be considered. As the differential operator L_λ acting on terms proportional V^2 gives zero, it does not occur in the transport relaxation equation for the scalar moments. Thus the tensorial expansion functions $\phi^r_{\mu\nu}\sim S^r_{5/2}{}^{-1}(V^2)\{V_\mu V_\nu\}^0$ are eigenfunctions of L_λ, and $\Gamma^{jk}_{\lambda}\sim\delta^{jk}$ for tensors of rank two. The operator $L_{\lambda\kappa}$ couples scalar moments to second rank tensors and vice versa. It has to be discussed in more detail later.

The first fourth rank tensor ($\sim\{\mathbf{VVVV}\}^0$) is an eigenfunction of $L_{\lambda\kappa}$ and, therefore, cannot couple via $\Gamma^{ij}_{\lambda\kappa}$ to the second rank tensors. As the matrix elements of the linear collision operator ω^{ij} couple tensors of equal rank only, it is the quadratic collision operator $\tilde{\omega}^{i,jk}$ alone, which couples fourth rank tensors to $\pi_{\mu\nu}$. In Ref. 6 it was shown that this coupling is negligible. The coupling was related to the occurrence of a normal pressure difference $(P_{zz}-P_{yy})$ in the plane normal to the flow. Computer simulations confirm that this does not occur even for shear rates beyond the applicability of the theory presented here. It is conjectured that the coupling of this fourth rank tensor to the other moments is also negligible. Hence, only scalar and tensorial moments of rank two are included.

The coupling via the quadratic collision operator is rather complex and will be neglected for the moment. When the results are presented in Sec. VI the modifications due to this coupling will also be discussed. Hence, at this stage, nonlinearities arise solely from the streaming term. The only second rank tensor considered in Ref. 6 is $\phi^1_{\mu\nu}$. Computer simulations give reason to include more tensorial expansion functions; thus here the influence of

$$\phi^2_{\mu\nu}\equiv\sqrt{4/7}(V^2-\tfrac{7}{2})\{V_\mu V_\nu\}^0 \tag{30}$$

and

$$\phi^3_{\mu\nu}\equiv\sqrt{4/63}(V^4-9V^2+\tfrac{63}{4})\{V_\mu V_\nu\}^0 \tag{31}$$

is studied.

In the Newtonian-flow regime the effect of $\phi^2_{\mu\nu}$ on the viscosity is rather small, for a Lennard-Jones gas at $T=2.75$ (in reduced units) the effect is less than 1%. Another extension is the inclusion of scalar expansion functions into the set of selected moments. The first two scalar expansion functions ($\phi^1=1$ and $\phi^2\sim V^2-\frac{3}{2}$) are collisional invariants and, due to (12), do not contribute; therefore,

$$\phi^3\equiv\sqrt{8/15}(\tfrac{1}{2}V^4-\tfrac{5}{2}V^2+\tfrac{15}{8}) \tag{32}$$

and

$$\phi^4\equiv\sqrt{16/35}(\tfrac{1}{6}V^6-\tfrac{7}{4}V^4+\tfrac{35}{8}V^2-\tfrac{35}{16}) \tag{33}$$

are the first two scalar expansion functions, whose effect on the velocity distribution is to be investigated in the following.

Before the chosen set of transport relaxation equations is finally written down, a few general relations for the Γ^{ij}_{λ} and $\Gamma^{jk}_{\lambda\kappa}$ terms are stated, which give an insight into the structure of the transport relaxation equations even beyond the closure chosen here. They can be derived using general relations for the Sonine polynomials:[17]

$$\omega_\lambda\langle L_\lambda(\phi^r_{\mu\nu})\phi^s_{\alpha\beta}\rangle a^{(s)}_{\alpha\beta}=2\{\epsilon_{\mu\lambda\kappa}\omega_\lambda a^{(s)}_{\kappa\nu}\}^0\delta^{rs}\ , \tag{34}$$

$$\gamma_{\lambda\kappa}\langle L_{\lambda\kappa}(\phi^r_{\mu\nu})\phi^s_{\alpha\beta}\rangle a^{(s)}_{\alpha\beta}=\{\gamma_{\mu\lambda}a^{(s)}_{\lambda\nu}\}^0\{\delta^{rs}[2+\tfrac{8}{7}(r-1)]+\delta^{s,r-1}\tfrac{4}{7}\sqrt{2(r-1)(2r+3)}\}\ , \tag{35}$$

$$\gamma_{\lambda\kappa}\langle L_{\lambda\kappa}(\phi^r_{\mu\nu})\phi^s\rangle a^{(s)}=\gamma_{\mu\nu}a^{(s)}\tfrac{1}{15}\sqrt{15(2r+3)}[\delta^{rs}\sqrt{2(2r+1)}+\delta^{s,r+1}2\sqrt{r}\,]\ , \tag{36}$$

$$\gamma_{\lambda\kappa}\langle L_{\lambda\kappa}(\phi^r)\phi^s_{\alpha\beta}\rangle a^{(s)}_{\alpha\beta}=\gamma_{\lambda\kappa}a^{(s)}_{\lambda\kappa}\frac{2}{\sqrt{15}}[\delta^{s,r-2}\sqrt{2(r-1)(r-2)}+\delta^{s,r-1}\sqrt{(r-1)(2r+1)}]\ . \tag{37}$$

Remember, $a^{(r)}=0$ for $r=1,2$. Hence, with (35) and (36) we conclude that the operator $L_{\lambda\kappa}$ couples $a^{(r)}_{\mu\nu}$ with the moment $a^{(r-1)}_{\mu\nu}$ and the two scalar moments $a^{(r)}$ and $a^{(r+1)}$. On the other hand, (37) expresses that the streaming term couples $a^{(r+1)}$ only with $a^{(r)}_{\mu\nu}$ and $a^{(r-1)}_{\mu\nu}$. Hence, with respect to the streaming term, the transport relaxation equations are closed. Only the matrix elements of the linear collision operator couple with higher-order moments. To close the system of equations this type of coupling to higher moments has to be neglected.

Finally, the following five equations are obtained (stationary state):

$$\omega^{11}\pi_{\mu\nu}+\omega^{12}a^{(2)}_{\mu\nu}+\omega^{13}a^{(3)}_{\mu\nu}+2\{\epsilon_{\mu\lambda\kappa}\omega_\lambda\pi_{\kappa\nu}\}^0+2\{\gamma_{\mu\lambda}\pi_{\lambda\nu}\}^0=-\sqrt{2}\gamma_{\mu\nu}\ , \tag{38}$$

$$\omega^{22}a^{(2)}_{\mu\nu}+\omega^{12}\pi_{\mu\nu}+\omega^{23}a^{(3)}_{\mu\nu}+2\{\epsilon_{\mu\lambda\kappa}\omega_\lambda a^{(2)}_{\kappa\nu}\}^0+\tfrac{22}{7}\{\gamma_{\mu\lambda}a^{(2)}_{\lambda\nu}\}^0+4\sqrt{2/7}\{\gamma_{\mu\lambda}\pi_{\lambda\nu}\}^0+14\sqrt{2/105}\gamma_{\mu\nu}a^{(3)}=0\ , \tag{39}$$

$$\omega^{33}a^{(3)}_{\mu\nu}+\omega^{23}a^{(2)}_{\mu\nu}+\omega^{13}\pi_{\mu\nu}+2\{\epsilon_{\mu\lambda\kappa}\omega_\lambda a^{(3)}_{\kappa\nu}\}^0+\tfrac{30}{7}\{\gamma_{\mu\lambda}a^{(3)}_{\lambda\nu}\}^0+\tfrac{24}{7}\{\gamma_{\mu\lambda}a^{(2)}_{\lambda\nu}\}^0+21\sqrt{2/105}\gamma_{\mu\nu}a^{(3)}+6/\sqrt{5}\gamma_{\mu\nu}a^{(4)}=0\ , \tag{40}$$

$$\omega^{33}_0a^{(3)}+\omega^{34}_0a^{(4)}+4/\sqrt{15}\gamma_{\lambda\kappa}\pi_{\lambda\kappa}+2\sqrt{14/15}\gamma_{\lambda\kappa}a^{(2)}_{\lambda\kappa}=0\ , \tag{41}$$

$$\omega^{44}_0a^{(4)}+\omega^{34}_0a^{(3)}+4/\sqrt{5}\gamma_{\lambda\kappa}a^{(2)}_{\lambda\kappa}+6/\sqrt{5}\gamma_{\lambda\kappa}a^{(3)}_{\lambda\kappa}=0\ . \tag{42}$$

For the scalar expansion functions the matrix elements of the linearized collision operator are denoted by ω_0^{rs}.

Note, the equation for the friction pressure (38) is only modified by terms involving nondiagonal parts of the collision matrix ω^{ij}. For Maxwell molecules these nondiagonal elements vanish, and they are small for a Lennard-Jones gas. For $T=2.75$, $\omega^{13}\cong 0.01\omega^{12}\cong 0.001\omega^{11}$; thus ω^{13} can be neglected. In any case, the effect of the additional moments on the friction pressure tensor and, therefore, on the viscosity coefficients, is small, a result which was to be expected since earlier computer simulation studies[12] showed satisfactory agreement of the viscosity coefficients with the results obtained in Ref. 6. However, for the velocity distribution function itself, all coefficients in the ansatz (13) contribute equally. For this purpose, our choice of moments seems to be the most complete one that can be calculated with reasonable effort.

A glance at Eqs. (35)–(37) indicates a hierarchy among the moments, at least for the coupling due to the streaming term. So there is some hope that the onset of nonlinear behavior on a microscopic level of description can be described using the approximation introduced above.

Some general remarks about our solution method seem to be appropriate at this point. Note, the highest order expansion functions, tensorial and scalar, involve V^6. In Grad's moment method[18] such terms can only stem from contractions of a tensor of rank 6. Hence, an equivalent calculation can be expected to be extremely cumbersome. Furthermore, it would involve much redundant information as only contractions, namely scalars and second rank tensors, are needed. The expansion with respect to irreducible tensors seems to be more appropriate for problems beyond the Burnett order.

IV. TRANSPORT RELAXATION EQUATIONS FOR THE COUETTE GEOMETRY

The transport relaxation equations (38)–(42) are now rewritten for the special Couette geometry: flow in x and shear gradient in y direction. Then, the irreducible second rank tensors have only three independent components: the xy component and two diagonal elements. It is useful to decompose them with respect to three orthonormal basis tensors $T^+_{\mu\nu}$, $T^-_{\mu\nu}$, and $T^0_{\mu\nu}$, defined by

$$T^+_{\mu\nu}\equiv\sqrt{2}\{e^x_\mu e^y_\nu\}^0 ,$$
$$T^-_{\mu\nu}=\frac{1}{\sqrt{2}}(e^x_\mu e^x_\nu - e^y_\mu e^y_\nu) , \tag{43}$$

$$T^0_{\mu\nu}\equiv\sqrt{3/2}\{e^z_\mu e^z_\nu\}^0 = \sqrt{2/3}[e^z_\mu e^z_\nu - \tfrac{1}{2}(e^x_\mu e^x_\nu + e^y_\mu e^y_\nu)] , \tag{44}$$

$e^{x,y,z}_\mu$ are the unit vectors in x,y,z direction, respectively. The corresponding components of the tensorial moments are introduced by, e.g.,

$$\pi_{\mu\nu}\equiv\pi_+ T^+_{\mu\nu}+\pi_- T^-_{\mu\nu}+\pi_0 T^0_{\mu\nu} \tag{45}$$

and analogously for $a^{(2)}_{\mu\nu}$ and $a^{(3)}_{\mu\nu}$.

Furthermore,

$$\gamma_{\mu\nu}\equiv\{\nabla_\mu v_\nu\}^0=\gamma\{e^x_\mu e^y_\nu\}^0 ,$$
$$\gamma\equiv\frac{\partial v_x}{\partial y} , \tag{46}$$

hence

$$\gamma_{\mu\nu}=\frac{\gamma}{\sqrt{2}}T^+_{\mu\nu} ,$$

and

$$\omega_\tau\equiv\tfrac{1}{2}\epsilon_{\tau\mu\nu}\nabla_\mu v_\nu=\frac{\gamma}{2}\epsilon_{\tau\mu\nu}e^y_\mu e^x_\nu=-\frac{\gamma}{2}e^z_\tau . \tag{47}$$

Some useful relations for the basis tensors are

$$T^i_{\mu\nu}T^j_{\mu\nu}=\delta^{ij} \quad \text{for } i,j=+,-,0 , \tag{48}$$

$$\{\epsilon_{\mu\lambda\kappa}e^z_\lambda T^k_{\kappa\nu}\}^0=-kT^{-k}_{\mu\nu} \quad \text{for } k=+,-,0 , \tag{49}$$

and

$$\sqrt{6}\{T^+_{\mu\lambda}T^+_{\lambda\nu}\}^0=-T^0_{\mu\nu}, \quad \{T^+_{\mu\lambda}T^-_{\lambda\nu}\}^0=0 ,$$
$$\sqrt{6}\{T^+_{\mu\lambda}T^0_{\lambda\nu}\}^0=-T^+_{\mu\nu} , \tag{50}$$

as can be verified easily.

Using these relations, Eqs. (38)–(42) can be rewritten in terms of the components of the tensors, Eqs. (51)–(61):

$$\Omega^{11}\pi_+-\Gamma\pi_--\frac{\Gamma}{\sqrt{3}}\pi_0+\Omega^{12}a^{(2)}_+=-\Gamma , \tag{51}$$

$$\Gamma\pi_++\Omega^{11}\pi_-+\Omega^{12}a^{(2)}_-=0 , \tag{52}$$

$$-\frac{\Gamma}{\sqrt{3}}\pi_++\Omega^{11}\pi_0+\Omega^{12}a^{(2)}_0=0 , \tag{53}$$

$$\Omega^{21}\pi_+-\sqrt{8/21}\Gamma\pi_0+\Omega^{22}a^{(2)}_+-\Gamma a^{(2)}_--\frac{11\Gamma}{7\sqrt{3}}a^{(2)}_0 +\Omega^{23}a^{(3)}_++\frac{14}{\sqrt{105}}\Gamma a^{(3)}=0 , \tag{54}$$

$$\Omega^{21}\pi_-+\Gamma a^{(2)}_++\Omega^{22}a^{(2)}_-+\Omega^{23}a^{(3)}_-=0 , \tag{55}$$

$$-\sqrt{8/21}\Gamma\pi_++\Omega^{21}\pi_0-\frac{11\Gamma}{7\sqrt{3}}a^{(2)}_+ +\Omega^{22}a^{(2)}_0+\Omega^{23}a^{(3)}_0=0 , \tag{56}$$

$$\Omega^{32}a^{(2)}_+-\tfrac{4}{7}\sqrt{3}\Gamma a^{(2)}_0+\Omega^{33}a^{(3)}_+-\Gamma a^{(3)}_- -\tfrac{5}{7}\sqrt{3}\Gamma a^{(3)}_0+\frac{21}{\sqrt{105}}\Gamma a^{(3)}+\sqrt{18/5}\Gamma a^{(4)}=0 , \tag{57}$$

$$\Omega^{32}a^{(2)}_-+\Gamma a^{(3)}_++\Omega^{33}a^{(3)}_-=0 , \tag{58}$$

$$\tfrac{4}{7}\sqrt{3}\Gamma a^{(2)}_++\Omega^{32}a^{(2)}_0-\tfrac{5}{7}\sqrt{3}\Gamma a^{(3)}_++\Omega^{33}a^{(3)}_0=0 , \tag{59}$$

$$\sqrt{8/15}\Gamma\pi_++\sqrt{28/15}\Gamma a^{(2)}_++\Omega^{33}_0a^{(3)}+\Omega^{34}_0a^{(4)}=0 , \tag{60}$$

$$\sqrt{8/5}\Gamma a^{(2)}_++\sqrt{18/5}\Gamma a^{(3)}_++\Omega^{43}_0a^{(3)}+\Omega^{44}_0a^{(4)}=0 . \tag{61}$$

The following abbreviations are used:

$$\tau^{-1}\equiv\omega^{11}, \quad \Gamma\equiv\gamma\tau, \quad \Omega^{ij}\equiv\omega^{ij}\tau, \quad \Omega^{ij}_0\equiv\omega^{ij}_0\tau . \tag{62}$$

τ is a characteristic relaxation time, Γ the reduced (dimensionless) shear rate. The matrix elements ω^{ij} and ω^{ij}_0

of the linear collision operator can be expressed in terms of the tabulated Chapman-Cowling integrals $\Omega^{(p,q)}$.[19] They must not be confused with the reduced matrix elements Ω^{ij} defined in (62). The tensorial elements ω^{ij} can be found in the literature.[2] For ω_0^{ij} one obtains

$$\omega_0^{33}=\tfrac{16}{15}n\,\Omega^{(2,2)}=\tfrac{2}{3}\omega^{11}\ , \tag{63}$$

i.e.,

$$\Omega_0^{33}\equiv\omega_0^{33}/\omega^{11}=\tfrac{2}{3}\ ,$$

$$\omega_0^{44}=\tfrac{2}{35}n\,(63\Omega^{(2,2)}-28\Omega^{(2,3)}+4\Omega^{(2,4)})\ , \tag{64}$$

$$\omega_0^{34}=\tfrac{4}{105}\sqrt{42}n(2\Omega^{(2,3)}-7\Omega^{(2,2)})\ , \tag{65}$$

for $T=2.75$, where τ defined in (62) happens to be equal to 1.001,

$$\Omega^{11}=1,\quad \Omega^{21}=\Omega^{12}=0.059,\quad \Omega^{22}=1.20\ ,$$

$$\Omega^{32}=\Omega^{23}=0.107,\quad \Omega^{33}=1.60\ ,$$

$$\Omega_0^{33}=\tfrac{2}{3},\quad \Omega_0^{43}=\Omega_0^{34}=\tfrac{2}{3}\sqrt{3}\Omega^{12}=0.068\ ,$$

$$\Omega_0^{44}=2\Omega^{22}-\tfrac{4}{3}=1.07\ .$$

Remember, $\{P_{\mu\nu}\}^0=\sqrt{2}P\pi_{\mu\nu}$, hence, the resulting viscosity coefficients in terms of the components of $\pi_{\mu\nu}$ read

$$\eta_+\equiv-\frac{1}{\gamma}P_{xy}=-\frac{P}{\gamma}\pi_+\ , \tag{66}$$

$$\eta_-\equiv-\frac{1}{2\gamma}(P_{xx}-P_{yy})=-\frac{P}{\gamma}\pi_-\ , \tag{67}$$

$$\eta_0\equiv-\frac{1}{2\gamma}[P_{zz}-\tfrac{1}{2}(P_{xx}+P_{yy})]=-\frac{\sqrt{3}}{2}\frac{P}{\gamma}\pi_0\ . \tag{68}$$

Neglecting all nonlinear terms in (51) and disregarding the coupling to higher moments one simply gets

$$\pi_+=-\Gamma,\quad \text{i.e.,}\quad \eta_+=P\tau\ , \tag{69}$$

the Newtonian limit.

If only the coupling to higher moments is disregarded the solution obtained in Ref. 6 follows, viz.,

$$\eta_+=\eta_B(1+\tfrac{2}{3}\Gamma^2)^{-1},\quad \eta_-=-\Gamma\eta_+,\quad \eta_0=\tfrac{1}{2}\Gamma\eta_+\ . \tag{70}$$

As Ω^{12} is small no remarkable effect of the higher moments on the viscosity coefficients can be expected. However, as will be seen later, they have to be included when the velocity distribution itself is regarded.

In Sec. VI it will be shown that $a_+^{(2)}$ and $a_+^{(3)}$ can be extracted from nonequilibrium molecular dynamics. The occurrence of these coefficients is not a pure nonlinear effect; e.g., if the transport relaxation equations (51)–(61) are linearized—with respect to deviations from local equilibrium—and solved for $a_+^{(2)}$ and $a_+^{(3)}$, one obtains

$$a_+^{(2)}\simeq-\frac{\Omega^{12}}{\Omega^{22}}\pi_+\simeq\frac{\Omega^{12}}{\Omega^{22}}\Gamma\simeq0.05\Gamma\ , \tag{71}$$

$$a_+^{(3)}=-\frac{\Omega^{23}}{\Omega^{33}}a_+^{(2)}\simeq-\frac{\Omega^{12}\Omega^{23}}{\Omega^{33}\Omega^{22}}\Gamma=-0.003\Gamma\ . \tag{72}$$

The scalar distortion, expressed by the coefficients $a^{(3)}$ and $a^{(4)}$, is a pure nonlinear effect.

Our intention is to compare the solution of the transport relaxation equations with results obtained from NEMD computer simulations. Section V will briefly introduce the method, and it is shown that the coupling behavior is modified due to the constant temperature constraint used in NEMD.

V. IMPLICATIONS OF THE MODEL SYSTEM

Given the pair potential of the particles, molecular dynamics simply consists of an integration of the Newtons equations of motion of N particles in a (cubic) box. In general, N is of the order of 100 to 1000, the present case is for $N=8^3=512$. To simulate quasimacroscopic systems periodic boundary conditions are employed.

To model a shear flow by nonequilibrium molecular dynamics, the periodic boundary conditions have to be modified, and several algorithms are at hand to generate a linear-flow profile.[20–22] The one used in this study is a minor modification of the method introduced by Evans,[23] using a sort of least-squares fit to adjust the flow field at every time step. The viscous heat is removed by simply rescaling the peculiar velocity of the particles. The equations of motion are integrated using a fifth-order predictor-corrector scheme.[20] The time evolution of the system is followed for some 10 000 timesteps and more, corresponding to about 1000 "collision times" (time between collisions).

In this way time averages of macroscopic quantities, such as the pressure tensor, shear modulus, etc., as well as of microscopic distribution functions, can be obtained. All these quantities are evaluated as N-particle averages at fixed timesteps and then time averaged. For the temperature, e.g., one has

$$\tfrac{3}{2}k_BT=\frac{m}{2}\frac{1}{N}\sum_{i=1}^{N}(\mathbf{c}^i-\mathbf{v})^2\ , \tag{73}$$

where $\mathbf{c}^i$ is the velocity of particle i. It is also interesting to note that the kinetic and potential contribution to the pressure tensor, and hence to the viscosity, can be extracted separately. In the following we focus on the kinetic part only, which is related to a distortion of the velocity distribution function.

In this study a Lennard-Jones system with density $n=0.1$ and temperature $T=2.75$ (in standard reduced units) is considered. This corresponds to an Argon gas at $T=330$ K and a pressure $P=12$ MPa, i.e., a fairly dense gas. The mean free path is $l\simeq3.2$. Despite these restrictions the system turns out to be a good, and computationally efficient, model for an ideal gas.

It is conjectured that this is due to the fact that the second Virial coefficient has its node (Boyle temperature) close to this state point; the potential contribution to the pressure is less than 2%. Some exploratory calculations have been performed with a density $n=0.01$ leading to the same results but consuming much more computer time. Data for the linear-flow regime at $T=1.2$ and $n=0.07$ have been presented in Ref. 5. The potential cutoff was set at the standard value $r=2.5$, and the integration stepwidth $\Delta t=0.005$ was used. Thirty-two

runs with a maximal number of 2400 timesteps were performed. The (pre)averages obtained from each run were again averaged over all 32 runs. The resulting standard deviations are displayed as error bars in the following plots. For the highest shear rates considered in this study only 400 timesteps for each of the 32 consecutive runs are needed to get a reasonable statistic. The simulations were performed on a Cray Research 1-M computer and, more recently, on a Cray Research XMP computer. It should be mentioned that the SLLOD algorithm[20,22] was also tested, leading to the same results.

The constant temperature constraint, inherent in most NEMD simulations, has drawn much attention in the last years.[14,24] A fluid undergoing viscous flow will usually heat up. To prevent this the simplest way is to rescale the velocities according to (73) after each integration step. An alternative can be derived from the Gauss principle, one of the most general principles of classical mechanics, which is also applicable to nonholonomic constraints. The exploitation of this principle for the constant temperature constraint leads to an additional nonconservative force in the equations of motion.[20] It is certainly interesting that the same force is necessary to guarantee $T=\text{const}$ for a Boltzmann gas undergoing viscous flow. The balance equation for the (kinetic) energy can be obtained from (16) if V^2 is substituted for ϕ^i:

$$\frac{d}{dt}\langle V^2\rangle+\sqrt{2}\gamma_{\mu\nu}\pi_{\mu\nu}-\sum_j\langle\tilde{K}_\lambda V_\lambda\phi^j\rangle a^j=2\langle\tilde{K}_\lambda V_\lambda\rangle\ . \tag{74}$$

The reduced force $\tilde{K}_\lambda$ is introduced by

$$K_\lambda\equiv\sqrt{2}mc_0\tilde{K}_\lambda\ . \tag{75}$$

For conservation of kinetic energy the simple ansatz

$$\tilde{K}_\lambda=-\beta V_\lambda \tag{76}$$

can be made. However, this choice is not unique. With the use of (12) and (46)–(48) β is determined from (74)

$$\beta=-\tfrac{1}{3}\gamma\pi_+\ . \tag{77}$$

Due to (69), one has $\beta>0$. At least for the purpose of comparison with the results of isothermal NEMD, this external force has to be included into the Boltzmann equation. The coupling behavior of this extra term can be treated in the same general way as in Sec. III. Two relations are useful,

$$V_\mu\frac{\partial}{\partial V_\mu}(\phi^r)=2(r-1)\phi^r+\sqrt{2(r-1)(2r-1)}\phi^{r-1}\ , \tag{78}$$

$$V_\mu\frac{\partial}{\partial V_\mu}(\phi^r_{\lambda\kappa})=2r\phi^r_{\lambda\kappa}+\sqrt{2(r-1)(2r+3)}\phi^{r-1}_{\lambda\kappa}\ . \tag{79}$$

Hence, the inhomogeneity term in (16) vanishes for all moments ($\langle\phi^i\rangle=0$), and the K^{ij} matrix elements (19) follow from (78), (79), and (14). They can be considered as modifications to the matrix elements of the linearized collision operator, see also Ref. 14. Both are combined to define a modified coupling element

$$\tilde{\Omega}^{ij}\equiv\Omega^{ij}+\tau K^{ij} \tag{80}$$

which substitutes for Ω^{ij} in the transport relaxation equations (51)–(61).

Note, the $\tilde{\Omega}^{ij}$ are no longer symmetric. They read

$$\begin{aligned}
&\tilde{\Omega}^{11}=\Omega^{11}+2\beta\tau,\quad \tilde{\Omega}^{12}=\Omega^{12}\ ,\\
&\tilde{\Omega}^{21}=\Omega^{21}+\sqrt{14}\beta\tau,\quad \tilde{\Omega}^{22}=\Omega^{22}+4\beta\tau\ ,\\
&\tilde{\Omega}^{23}=\Omega^{23},\quad \tilde{\Omega}^{32}=\Omega^{32}+6\beta\tau\ ,\\
&\tilde{\Omega}^{33}=\Omega^{33}+6\beta\tau\ ,\\
&\tilde{\Omega}^{33}_0=\Omega^{33}_0+4\beta\tau\ ,\tilde{\Omega}^{34}_0=\Omega^{34}_0\ ,\\
&\tilde{\Omega}^{43}_0=\Omega^{43}_0+\sqrt{42}\beta\tau,\quad \tilde{\Omega}^{44}_0=\Omega^{44}_0+6\beta\tau\ ,
\end{aligned} \tag{81}$$

for τ see Eq. (62). The hierarchy which was discussed for the coupling behavior of the streaming term is not affected by this addition; the higher moments still couple only via the (small) matrix element Ω^{12} to the viscosity.

VI. VISCOSITY COEFFICIENTS AND HIGHER MOMENTS

The transport relaxation equations (51)–(61) constitute a system of 11 coupled equations. For constant matrix elements Ω^{ij} the system is linear in the moments and its solution trivial. However, the modified matrix elements $\tilde{\Omega}^{ij}$ [Eq. (80)] depend on π_+ via β [Eqs. (76) and (77)]. Hence, the modified transport relaxation equations are solved self-consistently by an iterative scheme: the nth solution is obtained using β as calculated with the $(n-1)$st solution. The convergence is fast even when the matrix elements of the quadratic collision operator are included (see below).

To demonstrate the effect of the "thermostatic force" it is useful to neglect the coupling to higher moments and to consider Eqs. (51)–(53) only, i.e., the viscosity problem alone. The results are shown in Fig. 1. The dotted curves represent the results of Ref. 6, while the solid curve stems from the modification described above. The

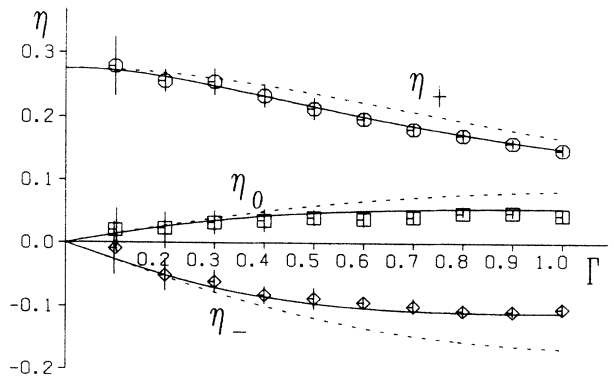

FIG. 1. Viscosity coefficients as functions of the reduced shear rate Γ for a Lennard-Jones gas at $T=2.75$ and $n=0.1$. Solution of the transport relaxation equations with the modification (80) (solid curves) and without (dotted curves) compared with NEMD results. The coupling of higher moments to the friction pressure is neglected (see text).

viscosity coefficients as obtained from NEMD were calculated according to (66)–(68) and the kinetic part of the pressure tensor, in turn, as indicated on the rhs of (29). The averages, of course, are evaluated as N-particle time averages in the simulation. In the same way the higher moments can be obtained from NEMD, cf. (15). The results compared with solutions of the modified transport relaxation equations are presented in Fig. 2. Note, the two moments $a_+^{(2)}$ and $a_+^{(3)}$ have a leading term linear in Γ, cf. (71) and (72), while the other, pure nonlinear, moments are divided by Γ^2 in the plots. These higher moments are even more sensitive to the inclusion of the extra force term. Hence, instead of comparing with the unmodified solution the influence of some quadratic collision matrix elements is exhibited. The dashed curves were calculated by considering the matrix elements of the linearized collision operator only. To get the full curves the transport relaxation equations (51)–(61) were again extended to include two matrix elements of the quadratic collision operator (16) and (18), viz.,

$$\tilde{\omega}^{2,11}=\tfrac{8}{245}\sqrt{7}n(\Omega^{(2,4)}-7\Omega^{(2,3)}+\tfrac{161}{12}\Omega^{(2,2)}) \tag{82}$$

and

$$\tilde{\omega}_3{}^{11}=\tfrac{8}{225}\sqrt{2}n\Omega^{(2,2)}=0.122\omega^{11} . \tag{83}$$

The matrix element $\tilde{\omega}^{2,11}$ couples $\{\pi_{\mu\lambda}\pi_{\lambda\nu}\}^0$ to $a_{\mu\nu}^{(2)}$, while $\tilde{\omega}_3{}^{11}$ couples $\pi_{\mu\nu}\pi_{\mu\nu}$ to the scalar moment $a^{(3)}$. With the decomposition (45) and the properties of the basis tensors (50) the additional term on the lhs of (54) reads

$$-\tfrac{1}{3}\sqrt{6}\tilde{\omega}^{2,11}\pi_+\pi_0 . \tag{84}$$

For (55) and (56) the corresponding terms are

$$-\tfrac{1}{3}\sqrt{6}\tilde{\omega}^{2,11}\pi_-\pi_0 \tag{85}$$

and

$$-\tfrac{1}{6}\sqrt{6}\tilde{\omega}^{2,11}(\pi_+^2+\pi_-^2-\pi_0^2) , \tag{86}$$

respectively. The matrix element $\tilde{\omega}_3{}^{11}$ leads to an extra contribution on the lhs of (60),

$$+\tilde{\omega}_3{}^{11}(\pi_+^2+\pi_-^2+\pi_0^2) . \tag{87}$$

It is cumbersome to calculate the other matrix elements for the quadratic collision operator. Nevertheless, these tedious calculations were carried out, but, only the two simple elements (82) and (83) are of a magnitude which cannot be neglected.

The agreement between data extracted from the simulations and solutions of the modified transport relaxation equations, as presented in Fig. 2, is satisfactory for almost the whole range of shear rates covered. For (reduced) shear rates greater than $\Gamma\cong 0.8$ higher moments, $a_{\mu\nu}^{(4)}$ and $a^{(5)}$, which are also evaluated in the simulation, increase remarkably, hence, they can no longer be neglected.

It should be pointed out again that for the viscosity problem neither the higher moments nor the quadratic collision operator need to be considered. They are needed to find an approximation for the velocity distribution function itself. In Sec. VII it will be shown how the full velocity distribution can be extracted from the NEMD simulation, independent of the moments considered so far. The approximate solution obtained from Eqs. (22) and (9) and the calculated moments displayed in Fig. 2 will be compared with the full distribution function. This will give indications about the quality of the closure chosen in Sec. III.

VII. VELOCITY DISTRIBUTION FUNCTIONS

To demonstrate how the velocity distribution function $F(\mathbf{V})$ can be obtained as a N-particle average, the following expansion is introduced:

$$F(\mathbf{V})=F^s(V^2)+F_{\mu\nu}^t(V^2)\{\hat{V}_\mu\hat{V}_\nu\}^0+\cdots . \tag{88}$$

F^s is the scalar, isotropic part, hence, using (22) and (9),

$$F^s(V^2)=F_M(V^2)(1+a^{(3)}\phi^3+a^{(4)}\phi^4+\cdots) . \tag{89}$$

The symmetric irreducible dyade $\{\hat{\mathbf{V}}\hat{\mathbf{V}}\}^0$ will be decomposed using the basis tensors $T_{\mu\nu}^+, T_{\mu\nu}^-, T_{\mu\nu}^0$ for the Couette symmetry. With the orthogonality relation (48) the tensorial product in (88) reads

$$\begin{aligned}F_{\mu\nu}^t(V^2)\{\hat{V}_\mu\hat{V}_\nu\}^0 \equiv{}& F^{(21)}(V^2)\hat{V}_x\hat{V}_y \\ &+\tfrac{1}{2}F^{(22)}(V^2)(\hat{V}_x\hat{V}_x-\hat{V}_y\hat{V}_y) \\ &+F^{(20)}(V^2)(\hat{V}_z\hat{V}_z-\tfrac{1}{3}) ,\end{aligned} \tag{90}$$

where $\hat{V}_{x,y,z}$ denotes the x,y,z component of the unit vector $\hat{\mathbf{V}}$ and the three partial distributions F^{21}, $F^{(22)}$, and $F^{(20)}$, corresponding to the three components of the moments, were introduced. Note,

$$(\hat{V}_z\hat{V}_z-\tfrac{1}{3})=\tfrac{2}{3}[\hat{V}_z\hat{V}_z-\tfrac{1}{2}(\hat{V}_x\hat{V}_x+\hat{V}_y\hat{V}_y)] . \tag{91}$$

Using the ansatz (75) and (77) the angular integration in (28) can be performed and for the xy component the result reads

$$P_{xy}=\frac{8\pi}{15}P\int F^{(21)}(V^2)V^4dV=-\eta_+(\gamma)\gamma , \tag{92}$$

i.e., there is a close relationship between the shear viscosity η_+ and the distribution function $F^{(21)}(V^2)$.

The same holds true for $F^{(22)}$ and η_- and $F^{(20)}$ and η_0, respectively,

$$\begin{aligned}\tfrac{1}{2}(P_{xx}-P_{yy})&=\frac{8\pi}{15}P\int F^{(22)}(V^2)V^4dV \\ &=-\eta_-(\gamma)\gamma ,\end{aligned} \tag{93}$$

$$\begin{aligned}\tfrac{1}{2}[P_{zz}-\tfrac{1}{2}(P_{xx}+P_{yy})]&=\frac{8\pi}{15}P\int F^{(20)}(V^2)V^4dV \\ &=-\eta_0(\gamma)\gamma .\end{aligned} \tag{94}$$

As the friction pressure P_{xy} is nonvanishing even in the Newtonian regime, one can try to detect $F^{(21)}$ for low shear rates. Shear thinning should appear as a deformation of $F^{(21)}$ in a way that the integral (92) leads to lower values for P_{xy}.

The occurrence of the distribution functions $F^{(20)}$ and

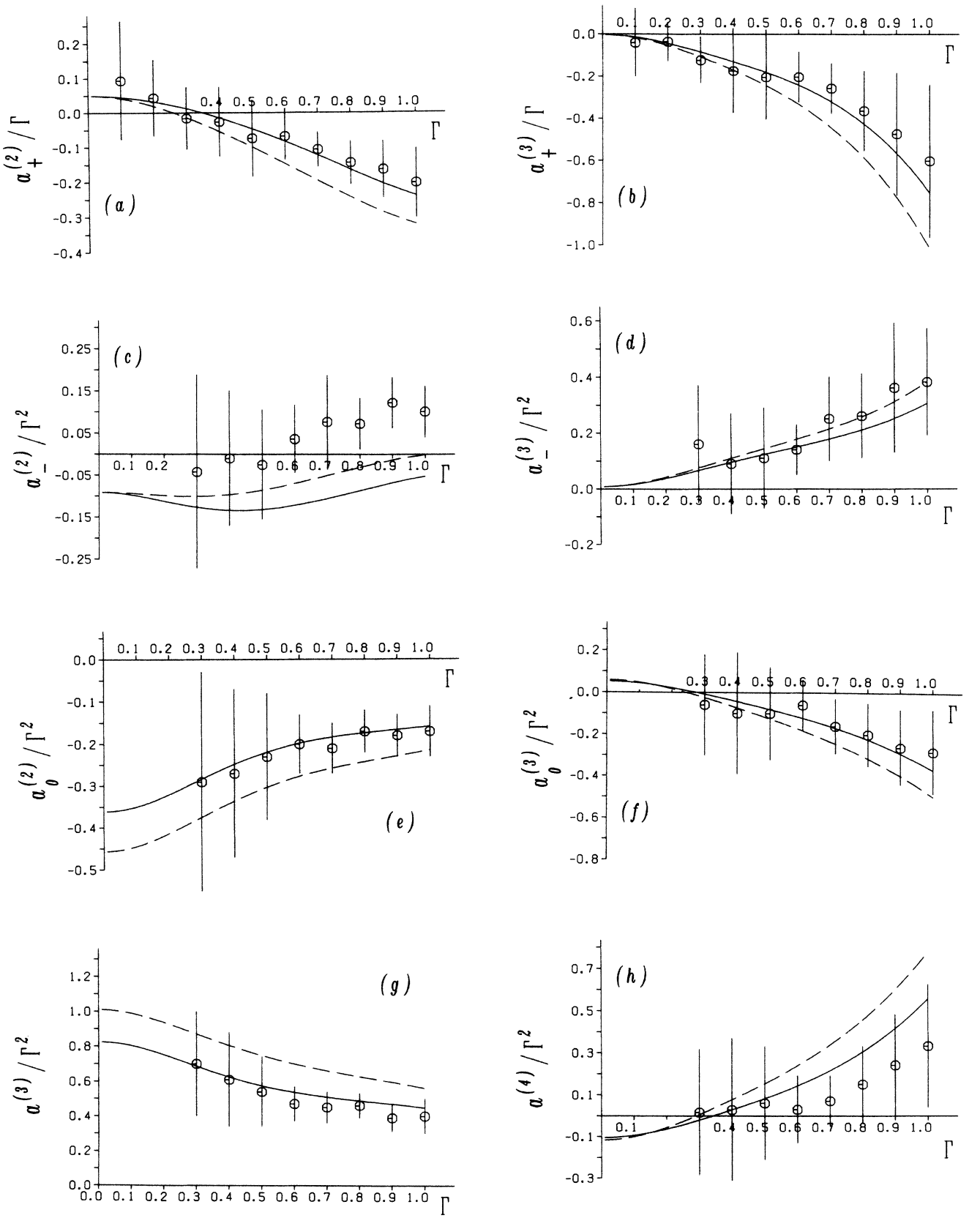

FIG. 2. The shear-rate dependence of the higher moments. Solutions of the modified transport relaxation equations [Eqs. (51)–(61)] are compared with NEMD results (dashed curves). To obtain the solid curves the two relevant matrix elements of the quadratic collision operator [Eqs. (82) and (83)] were considered in addition.

$F^{(22)}$, on the other hand, is a pure nonlinear effect, related to normal pressure differences. The relation to the expansion (22) is the following:

$$F^t_{\mu\nu}(V^2)\{\hat{V}_\mu\hat{V}_\nu\}^0=F_M(V^2)(\pi_{\mu\nu}\phi^1_{\mu\nu}+a^{(2)}_{\mu\nu}\phi^2_{\mu\nu}+a^{(3)}_{\mu\nu}\phi^3_{\mu\nu}+\cdots)\,. \quad (95)$$

Using (45) and (95), the definition

$$\phi^r_{\mu\nu}\equiv|\phi^r|\{\hat{V}_\mu\hat{V}_\nu\}^0 \quad (96)$$

and the expansion

$$\{\hat{V}_\mu\hat{V}_\nu\}^0=\sqrt{2}\hat{V}_x\hat{V}_yT^+_{\mu\nu}+\sqrt{1/2}(\hat{V}^2_x-\hat{V}^2_y)T^-_{\mu\nu}+\sqrt{3/2}(\hat{V}^2_z-\tfrac{1}{3})T^0_{\mu\nu}\,, \quad (97)$$

one finally ends up with

$$F^{(21)}(V^2)=\sqrt{2}F_M(V^2)(\pi_+|\phi^1|+a^{(2)}_+|\phi^2|+a^{(3)}_+|\phi^3|+\cdots)\,, \quad (98)$$

$$F^{(22)}(V^2)=\sqrt{2}F_M(V^2)(\pi_-|\phi^1|+a^{(2)}_-|\phi^2|+a^{(3)}_-|\phi^3|+\cdots)\,, \quad (99)$$

$$F^{(20)}(V^2)=\sqrt{3/2}F_M(V^2)(\pi_0|\phi^1|+a^{(2)}_0|\phi^2|+a^{(3)}_0|\phi^3|+\cdots)\,. \quad (100)$$

Note, that the $|\phi^i|$ are known functions of V^2; e.g., with (27), (30), (31), and (96) one gets

$$|\phi^1|=\sqrt{2}V^2,\quad |\phi^2|=\tfrac{2}{7}\sqrt{7}(V^2-\tfrac{7}{2})V^2\,,$$
$$|\phi^3|=\tfrac{2}{21}\sqrt{7}(V^4-9V^2+\tfrac{63}{4})V^2\,. \quad (101)$$

The (partial) distribution functions F^s, $F^{(21)}$, $F^{(22)}$, and $F^{(20)}$ are N-particle averages of

$$\sum_i\delta(V-V^i),\quad \sum_i\hat{V}_x\hat{V}_y\delta(V-V^i)\,,$$
$$\sum_i\tfrac{1}{2}(\hat{V}^2_x-\hat{V}^2_y)\delta(V-V^i)\,,$$

and

$$\sum_i(\hat{V}^2_z-\tfrac{1}{3})\delta(V-V^i)\,,$$

respectively.

For their calculation the "essential" part of the velocity space is divided into 64 spherical shells. In these shells the above averages are evaluated, thus the distribution functions are obtained at 64 points. The number of particles in the shells will be proportional to $V^2\exp(-V^2)$; hence, a limiting radius can be found, assuring that "almost all" particles are included, e.g., 98% of the particles have speeds with $V^2\leq 5$. But, the few faster particles contribute considerably to the momentum transport, hence, they must not be neglected. Note, the integrand in (92)–(94) is proportional to V^4. Therefore, one has to extend the limiting radius as far as is consistent with a reasonable statistic for each shell.

Before this discussion is continued, it is shown how the δ-function averages can be transformed in a numerically tractable form; ΔN_j denotes the mean number of particles in the jth shell, and (ΔV_j^2) is the corresponding speed interval covered. The normalization condition (6) can be written as, cf. (88),

$$\frac{1}{N}\sum_{j=1}^{64}(\Delta N_j)\cong 1=\int F(\mathbf{V})d^3V$$
$$=2\pi\int_0^\infty F^s(V^2)Vd(V^2)$$
$$\cong 2\pi\sum_{j=1}^{64}\int_{(\Delta V_j^2)}F^s(V^2)Vd(V^2)$$
$$=\sum_{j=1}^{64}2\pi F^s(\bar{V}^2_j)\bar{V}_j(\Delta V^2_j)\,. \quad (102)$$

In the last manipulation the mean value theorem has been used. For each shell j one obtains

$$F^s(\bar{V}^2_j)=\frac{(\Delta N_j)}{2\pi\bar{V}_j(\Delta V^2_j)N}\,. \quad (103)$$

In order to achieve good statistics for the few fast particles, the intervals are chosen such that on the average the particles are equally distributed among the shells.

This turns out to be essential for the following. In this way the intervals for very low speeds ($V^2<0.2$), as well as for high speeds ($V^2>2.5$) get broader, thus the mean value theorem should be evaluated exactly. This was done numerically, assuming that F^s does not deviate strongly from the Maxwellian distribution. Finally, the limiting radius was $V^2=8.6$ and on the average only less than 0.1% of the particles are not included in this sphere. For the other distribution functions the same intervals and grid points were used. Aside from some normalization factors, which arise from the angular integration, they are obtained in the same way as the isotropic part.

Figure 3 shows the scalar part $F^s(V^2)$ for $\gamma=0.1$, reproducing the Maxwellian distribution with high accuracy. Another measure of the quality of the scalar distribution function can be obtained when F^s is used to calculate the normalization integral (6) and the temperature according to (7). The agreement is perfect.

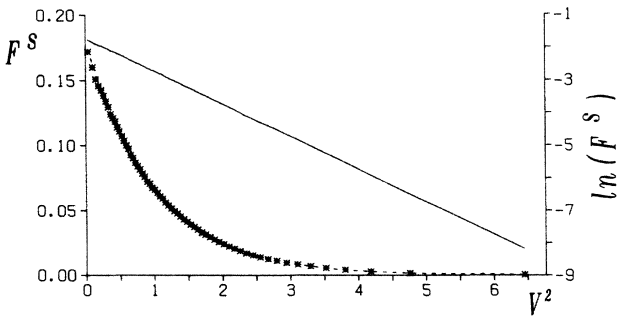

FIG. 3. The scalar part F^s of the velocity distribution function for the shear rate $\gamma=0.1$ (linear-flow regime) compared with the Maxwellian distribution (dashed curve). The straight line refers to the logarithmic scale.

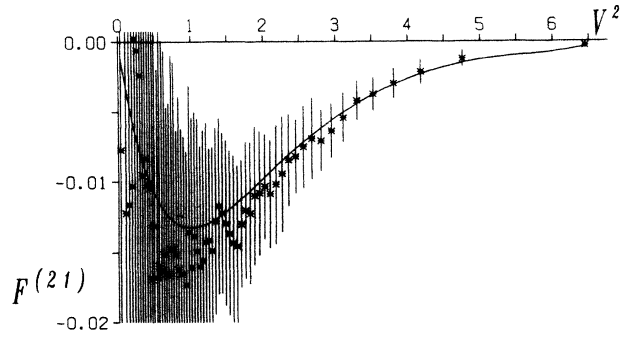

FIG. 4. The partial distribution function $F^{(21)}$ for the shear rate $\gamma=0.1$ (linear-flow regime) compared with the linear theory, cf. Eq. (104).

The tensorial distribution functions, being nonequilibrium properties, cannot be extracted in this quality. Figure 4 shows $F^{(21)}(V^2)$ for the same shear rate. Thirty-two runs with 2400 timesteps each were performed. The results of each run were recorded, thus the curves plotted are averages of the 32 runs. The standard deviations are shown as error bars in the plot. The result is compared with the linear theory, i.e.,

$$\pi_+=-\gamma\tau \quad \text{and} \quad F^{(21)}(V^2)=-2F_M(V^2)V^2\gamma\tau \ . \tag{104}$$

When the distribution function $F^{(21)}$ is used to evaluate the friction pressure P_{xy} the agreement is 99%. This is due to the smoothing of the integration and to the fact that the slow particles, for which the statistical error is maximal, do not contribute noticeably to the integral.

VIII. MICROSCOPIC ORIGIN OF NON-NEWTONIAN FLOW BEHAVIOR

When the shear rate is increased, nonlinear effects can no longer be neglected in the discussion of the velocity distribution function. They are related to non-Newtonian behavior on a macroscopic scale, e.g., shear thinning and normal pressure differences. Figure 5 shows $F^{(21)}$ for $\gamma=0.5$, again compared with the linear theory (dashed curve) and the nonlinear theory presented in the preceding sections (solid curve). Especially for higher speeds, which are important for the momentum transport, the deviations from the linear theory are most pronounced. Shear thinning is clearly visible in a distortion of the corresponding distribution function. Evaluating the integral (92) using $F^{(21)}$ gives the explicitly extracted mean value of P_{xy} up to 4%, which is less than the standard deviation of this quantity.

More appropriate to compare with our nonlinear theory is a presentation such as in Fig. 6, where $F^{(21)}/F_M$ is plotted for the same shear rate $\gamma=0.5$. Even for lower shear rates it reveals the occurrence of higher order polynomials in the expansion (98), corresponding to the coefficients π_+, $a_+^{(2)}$, and $a_+^{(3)}$. Insertion of the calculated moments gives the solid curve in Fig. 6. The agreement is again excellent even in this very sensitive presentation.

The same holds for the scalar part F^s, whose deviation from the Maxwellian distribution was not to be expected. Indeed, the results presented here motivated the consideration of the scalar moments in the moment method. For $\gamma=0.1$ (Fig. 3) no deviation from the Maxwellian shape occurred. For $\gamma=0.3$ (Fig. 7) the logarithmic scale reveals a small deviation in the tail of the distribution. If (F^s/F_M-1) is plotted (Fig. 8), the result should have $a^{(3)}\phi^3$ as the leading term. Indeed, one gets a reasonable fit for the data with the polynomial $\phi^3(V^2)$ and the calculated coefficient $a^{(3)}$ alone. Again, the tail of the Maxwellian distribution was of great importance. Considering the small absolute values of F^s or $F^{(21)}$ for $V^2>4$ (Figs. 5 and 7), it is surprising how accurately the simulation reveals the interesting effects of these few and fast particles. Note, the distortion of the directionally averaged scalar part of the distribution function couples only indirectly, via the second tensorial moment, to the friction pressure, cf. (38) and (39).

The distribution functions $F^{(22)}$ and $F^{(20)}$, being pure nonlinear entities, cannot be extracted in this quality. For the shear reate $\gamma=1.0$ they are displayed in Fig. 9. These distortions of the velocity distribution function resemble the occurrence of normal pressure differences in the gas. The evaluation of the integrals (93) and (94) gives viscosity coefficients η_- and η_0 which deviate by 8% and 14%, respectively, from the mean values extract-

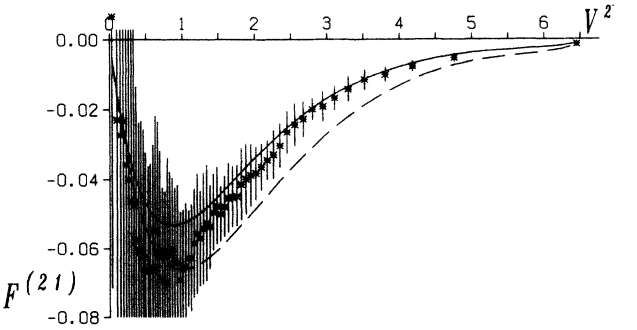

FIG. 5. The partial distribution function $F^{(21)}$ for the shear rate $\gamma=0.5$ (nonlinear-flow regime). Comparison of NEMD results with nonlinear (solid curve) and linear theory (dashed curve).

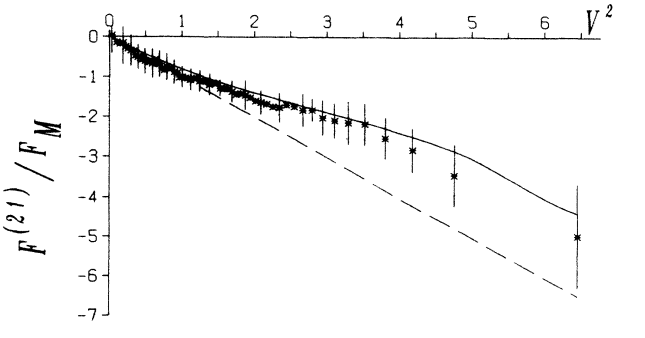

FIG. 6. The partial distribution function $F^{(21)}$ of Fig. 5 divided by the Maxwellian distribution, cf. (98). Comparison of linear theory [dashed curve, cf. (104)] and nonlinear theory (solid curve).

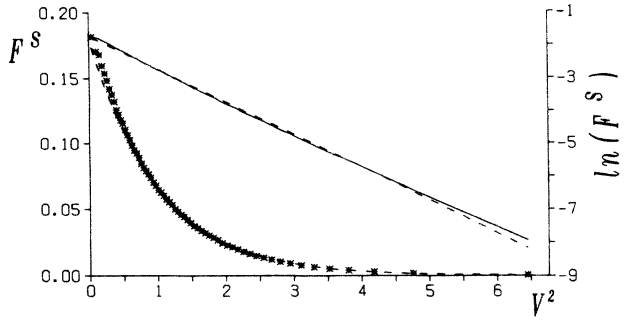

FIG. 7. The scalar part F^s of the velocity distribution function for the shear rate $\gamma=0.3$ (nonlinear-flow regime) compared with the Maxwellian distribution (dashed curve). Small deviations occur on the logarithmic scale.

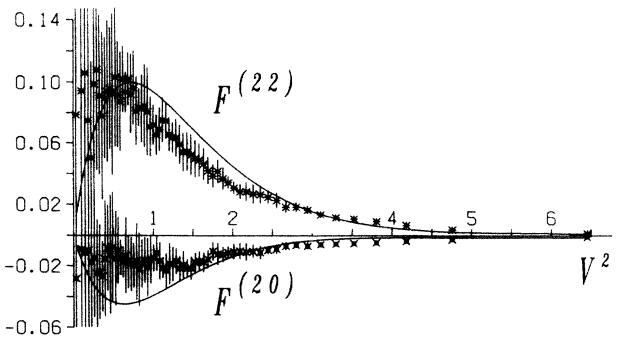

FIG. 9. The partial distribution functions $F^{(22)}$ and $F^{(20)}$ for the shear rate $\gamma=1.0$, cf. (99) and (100). The occurrence of these distortions is a pure nonlinear effect and related to normal pressure differences, cf. (93) and (94).

ed explicitly from the simulation.

The limitation of the closure chosen in this work to shear rates $\gamma<0.8$ is apparent in Fig. 9 as well as in Fig. 2. But, at least qualitatively, agreement with predictions of the theory presented can be observed.

IX. CONCLUDING REMARKS

The closure of the transport relaxation equations chosen in this article is appropriate to approximate the velocity distribution function for a Couette flow far from equilibrium. The agreement between predictions of kinetic theory and results from NEMD computer simulations is excellent provided that a "thermostatic force," inherent in most NEMD calculations, is taken into account explicitly. The conclusions that can be drawn out of this study are twofold.

Concerning the kinetic theory of gases, which is more than 100 years old, new light is shed on solution methods for flow far from equilibrium. The moment method as used in this work turned out to be more suitable for problems beyond the 13-moment description than, e.g., Grad's method.[18] It is shown that for the viscosity problem alone higher moments as well as the quadratic part of the collision operator can be neglected. However, they

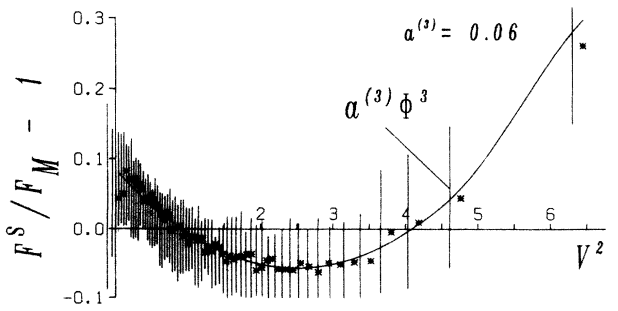

FIG. 8. The deviation of the scalar part F^s of the velocity distribution function from the Maxwellian shape for the shear rate $\gamma=0.3$, cf. (89). The coefficient $a^{(3)}$ stems from the solution of the modified transport relaxation equations.

are essential to approximate the velocity distribution function.

NEMD, on the other hand, can still be considered to be in its exploratory stage. Generally, it is aimed to mimic the corresponding "real" experiment as closely as possible. In its first decade transport properties of liquids as obtained from the simulations were compared to experimental data. Kinetic gas theory based on the Boltzmann equation offers a well-probed and well-established description for the velocity distribution function. The results obtained from the exploitation of the moment method provide a test for the simulation even on a microscopic level of description. The excellent agreement of the two approaches used in this work lead us to the conclusion that NEMD can indeed provide a valuable supplementary "experiment," especially in domains where current laboratory facilities fail.

Of course, constraints used in the simulation have to be taken into account. So far, their effect on the underlying kinetic equation was generally neglected. In this study the explicit inclusion of the "thermostatic force" in the Boltzmann equation was essential.

The work presented here encourages one to study boundary effects of gas flow. Again, a theory to describe the flow close to a boundary is at hand.[25] The moment method and thermodynamical concepts are invoked to solve the Boltzmann equation with boundary conditions. In Ref. 26 the heat-conduction problem between parallel plates was solved using this theory. It is interesting to note, that the scalar moment $a^{(3)}$ was considered in Ref. 26.

It is conjectured that for the Couette flow too, one has to include more than the commonly used 13 moments to describe the flow field close to the boundary. Following the line of this paper a combined approach using both nonequilibrium molecular dynamics and the theoretical concepts mentioned above seems to be promising.

Note added. An analytic formula for the shear-rate dependence of the viscosity coefficients as discussed in Sec. VI (Fig. 1) has been derived recently.[27] It perfectly fits the NEMD data even up to the (reduced) shear rate $\Gamma=10$.

[1]L. Waldmann, *Transporterscheinungen in Gasen von mittlerem Druck,* Vol. 12 of *Handbuch der Physik,* edited by S. Flügge (Springer, Berlin, 1959), p. 295.

[2]S. Chapman and T. G. Cowling, *The Mathematical Theory of Non-Uniform Gases* (Cambridge University Press, Cambridge, 1939).

[3]S. Hess and A. Mörtel, Z. Naturforsch., Teil A **32**, 1239 (1977).

[4]F. Baas, P. Oudeman, H. F. P. Knaap, and J. J. M. Beenakker, Physica **89A**, 73 (1977); B. S. Douma, H. F. P. Knaap, and J. J. M. Beenakker, Chem. Phys. Lett. **74**, 421 (1980).

[5]W. Loose and S. Hess, Phys. Rev. Lett. **58**, 2443 (1987).

[6]N. Herdegen and S. Hess, Physica **115A**, 281 (1982).

[7]D. J. Evans, H. J. M. Hanley, and S. Hess, Phys. Today (No. 1) **37**, 26 (1984), and other articles in this special issue dealing with fluids out of equilibrium.

[8]*Nonlinear Fluid Behavior,* Proceedings of the Conference on Nonlinear Fluid Behavior, University of Colorado, Boulder, 1982, edited by H. J. M. Manley [Physica **118A** (1983)].

[9]S. Hess, Phys. Rev. A **22**, 2844 (1980).

[10]S. Hess, Phys. Rev. A **25**, 614 (1982); J. C. Rainwater and S. Hess, Physica **118A**, 371 (1983); H. M. Koo and S. Hess, *ibid.* **145A**, 361 (1987).

[11]R. Zwanzig, J. Chem. Phys. **71**, 4416 (1979); B. C. Eu, *ibid.* **74**, 3006 (1981); D. M. Heyes and R. Szczepanski, J. Chem. Soc. Faraday Trans. 2 **83**, 319 (1987).

[12]S. Hess, H. J. M. Hanley, and N. Herdegen, Phys. Lett. **105A**, 238 (1984).

[13]D. J. Evans, Physica **118A**, 51 (1983).

[14]J. W. Dufty, A. Santos, J. J. Brey, and R. F. Rodriguez, Phys. Rev. A **33**, 459 (1986); J. W. Dufty, J. J. Brey, and A. Santos, in *Proceedings of the International School of Physics Enrico Fermi, Course XCVII, Molecular-Dynamics Simulation of Statistical Mechanical Systems,* edited by G. Ciccotti and W. G. Hoover (North-Holland, Amsterdam, 1986).

[15]A. J. C. Ladd and W. G. Hoover, J. Stat. Phys. **38**, 973 (1985).

[16]S. Hess and W. Köhler, *Formeln zur Tensorrechnung* (Palm & Enke, Erlangen, 1980).

[17]I. S. Gradshteyn and I. M. Ryzhik, *Table of Integrals, Series, and Products* (Academic, New York, 1980).

[18]H. Grad, in *Principles of the Kinetic Theory of Gases,* Vol. 12 of *Handbuch der Physik,* edited by S. Flügge (Springer, Berlin, 1959), p. 205; Commun. Pure Appl. Math. **2**, 331 (1949).

[19]J. Hirschfelder, C. Curtiss, and R. Bird, *Molecular Theory of Gases and Liquids* (Wiley, New York, 1954).

[20]D. J. Evans and G. P. Morris, Comp. Phys. Rep. **1**, 297 (1984).

[21]W. G. Hoover, *Molecular Dynamics* (Springer, Berlin, 1986); Annu. Rev. Phys. Chem. **34**, 103 (1983); Physica **118A**, 111 (1983).

[22]D. J. Evans and W. G. Hoover, Annu. Rev. Fluid Mech. **18**, 243 (1986).

[23]D. J. Evans, Mol. Phys. **37**, 1745 (1979).

[24]D. J. Evans and G. P. Morris, Phys. Rev. Lett. **56**, 2172 (1986).

[25]L. Waldmann and H. Vestner, Physica **99A**, 1 (1979).

[26]H. Vestner and L. Waldmann, Z. Naturforsch., Teil A **32**, 667 (1977).

[27]W. Loose, Phys. Lett. A (to be published).